Available online at www.sciencedirect.com
SCIENCE DIRECT®
International Journal of Mass Spectrometry 236 (2004) 105–116
International Journal of Mass Spectrometry
www.elsevier.com/locate/ijms

$C_4H_8^{\bullet+}$ isomerizations by theory

Charles E. Hudson, David Wang, David J. McAdoo*

Department of Neurosciences and Cell Biology, University of Texas Medical Branch, 301 University Boulevard, Galveston, TX 77555–1043, USA

Received 4 March 2004; accepted 7 June 2004

Available online 23 July 2004

Abstract

Structures, energies and reaction coordinates for much of the $C_4H_8^{\bullet+}$ potential surface were obtained by ab initio and density functional theories. Most $C_4H_8^{\bullet+}$ isomers are demonstrated to be mutually accessible below the threshold for the lowest energy dissociation, consistent with inferences from earlier experimental data. The "virtual intermediates" (point that reactions pass through corresponding to a conventional structure but lacking a corresponding potential minimum) $CH_3^+CHCH_2CH_2^\bullet$ and $^+CH_2CH(CH_3)CH_2^\bullet$ are found to be very important in $C_4H_8^{\bullet+}$ rearrangements. $CH_3^+CHCH_2CH_2^\bullet$ is accessed from the 1-butene cation by a 1,4- and a 1,2-H-shift, the 2-butene cation by a 1,2-H-shift and the 1-methylcyclopropane cation by ring opening. All reactions through $CH_3^+CHCH_2CH_2^\bullet$ begin or end with a 1,2-H-shift going to or from the 1-butene ion. The 1-butene cation appears to form rather than the more stable 2-butene cation because the minimum energy pathways down from higher energy transition states go to the 1-butene cation side of the transition state that connects the 1-butene and the 2-butene ions. Perhaps charge localization on the CH carbon directs these pathways to the 1-butene cation by a carbocation-like rearrangement. Predicted competition between 1,3- and consecutive 1,2-transfers across double bonds, despite 1,2-shifts being energetically strongly favored over 1,3-shifts in other systems, is another interesting feature of $C_4H_8^{\bullet+}$ reactions. The lowest energy isomerization found in this work was a 1,5-H-shift in the 1-pentene ion. In contrast to $CH_3^+CH\ CH_2CH_2^\bullet$, $CH_3^+CHCH_2CH_2CH_2^\bullet$ appears to inhabit a potential energy minimum, albeit a shallow one. The order of the critical energies for different ring sized transfers is 1,4 > 1,3 ≅ 1,2 > 1,5 in the $C_nH_{2n}^{\bullet+}$ ions examined, differing from the order 1,3 > 1,4 > 1,2 > 1,5 established for other homologous series of aliphatic radical cations.

Keywords: Ab initio; $C_4H_8^{\bullet+}$; $C_5H_{10}^+$; Distonic ions; Rearrangements; Virtual intermediates

1. Introduction

$C_4H_8^{\bullet+}$ dissociations have been extensively utilized to investigate the dynamics of unimolecular dissociations [1–5]. However, $C_nH_{2n}^{\bullet+}$ isomerizations are less understood than those of most other radical cations because extensive isotopic exchange and loss of distinction prior to dissociation obscure the details of $C_nH_{2n}^{\bullet+}$ reactions. McLafferty and coworkers [6] concluded from differences among collisionally activated dissociations of $C_4H_8^{\bullet+}$ ions derived from different neutral precursors that isomerization is limited below the threshold for $C_4H_8^{\bullet+}$ dissociation. However, Smith and Williams [7] observed common metastable dissociation spectra of $C_4H_8^{\bullet+}$ and $C_6H_{12}^{\bullet+}$ isomers; Lin and Harrison [8] found extensive redistribution of labels in the low energy dissociations of ^2H and ^{13}C-labeled 2-methylpropene ions; Meisels and coworkers [9,10] demonstrated that the ions generated from the six C_4H_8 isomers have indistinguishable breakdown graphs near threshold, and five $C_4H_8^{\bullet+}$ isomers display identical dissociation rates [1]. All of this indicates loss of identity of the isomers by extensive rearrangement at low energies. However, some distinctness of electron impact spectra, particularly for methylcyclopropane and cyclobutane cations, suggests decomposition from specific structures at high energies [8]. This likely reflects more rapid increases in rates of simple bond cleavages than of isomerizations with increasing internal energy.

McFadden attributed the occurrence of considerable H/D exchange in deuterated propene ions to their 1 and 3 positions being rendered equivalent by a series of 1,3-H-shifts [11]. In contrast, Millard and Shaw [12] concluded that hydrogen atoms rearrange by a series of 1,2-H shifts in $C_4H_8^{\bullet+}$ and $C_5H_{10}^{\bullet+}$ ions. They also concluded that 1,5-H-transfer does not precede most ethene loss from the 1-pentene ion

* Corresponding author. Tel.: +1 409 772 2939; fax: +1 409 772 3222.
E-mail address: djmcadoo@utmb.edu (D.J. McAdoo).

1387-3806/$ – see front matter © 2004 Elsevier B.V. All rights reserved.
doi:10.1016/j.ijms.2004.06.003

because deuterium labeling indicated preferential ethene loss from the unsaturated end of that ion. Lin and Harrison [8] proposed skeletal isomerization by 1,3-ring closures to form methylcyclopropane ions followed by reopening, making both 1,2 and 1,3 H-shifts unnecessary, although not precluding them. Theory reveals that the propene ion undergoes degenerate isomerization via both a 1,3-H-shift [13] and by two consecutive 1,2-H-shifts [14,15] in which the trimethylene radical cation may be a distinct intermediate. However, the shallowness of the well (ca. 1 kJ mol^{-1} deep) and the low level MP2 theory applied make this uncertain. Nonetheless, these results for $C_3H_6^{\bullet+}$ rearrangements suggest that both McFadden and Millard and Shaw were partly right. The novelty of these reactions and the absence of their study in higher $C_nH_{2n}^{\bullet+}$ ions make their further characterization of interest. Scheme 1 summarizes $C_4H_8^{\bullet+}$ interconversions to be studied here and gives the numerical labels that are used to designate each isomer. Jungwirth and Bally [16] generated a reasonable $C_4H_8^{\bullet+}$ potential surface by combining their results with thermochemical data and estimating some energies from theoretical results for $C_3H_6^{\bullet+}$ [15]. However, they did not directly characterize some reactions of uppermost present interest, 1,2- and 1,3-H-shifts (**1** → **2**), a 1,2-methyl shift (**1** → **3**) and ring openings/cyclizations (**1** → **4** and **3** → **5**). Therefore, we examined the reactions of $C_4H_8^{\bullet+}$ and some $C_5H_{10}^{\bullet+}$ ions by ab initio theory, including intrinsic reaction coordinate (IRC) tracing [17,18], an approach that often reveals novel features of reaction coordinates inaccessible by other means [19–22].

2. Theory

All calculations were performed by unrestricted theories using the Gaussian 98W package of programs [23]. $C_4H_8^{\bullet+}$ geometries were obtained by B3LYP/6-31G(d,p) hybrid functional and QCISD/6-31G(d,p) ab initio theories. B3LYP/6-31G(d,p), QCISD/6-31G(d,p), QCISD(T)/6-311-G(d,p) and PMP3/6-311G(d,p) theories were used to obtain energies for $C_4H_8^{\bullet+}$ stationary points; QCISD(T) and PMP3 energies were obtained at QCISD/6-31G(d,p) geometries. $C_5H_{10}O^{\bullet+}$ structures were characterized at the same levels of theory as $C_4H_8^{\bullet+}$ species, except at QCISD/6-31G(d) in place of QCISD/6-31G(d,p) theory. Zero point energies were obtained by B3LYP/6-31G(d,p) theory and are unscaled. Transition states were all characterized by having only one imaginary frequency. Values of s^2 were close to the ideal value of 0.75 for ground states and B3LYP transition states (only **4** and **5** gave values as high as 0.78 for any stable species, and only the methyl shift **1** → **1″** gave a value as high as 0.78 for any B3LYP/6-31G(d,p) transition state. However, for QCISD (UHF theory) transition states, s^2 values ranged from 0.76 (**4** → **1**) to 0.96 (**1** → **1″**). Projecting out the contributions of states $s + 1$ to $s + 4$ with PMP3 computations gave s^2 values of 0.7500 for all stationary points at their QCISD/6-31G(d,p) geometries. However, this projection had little effect on the energies obtained (Table 2). Degrees of bonding were assessed by Mulliken overlap population analyses. Reaction trajectories were characterized by intrinsic reaction coordinate (IRC)

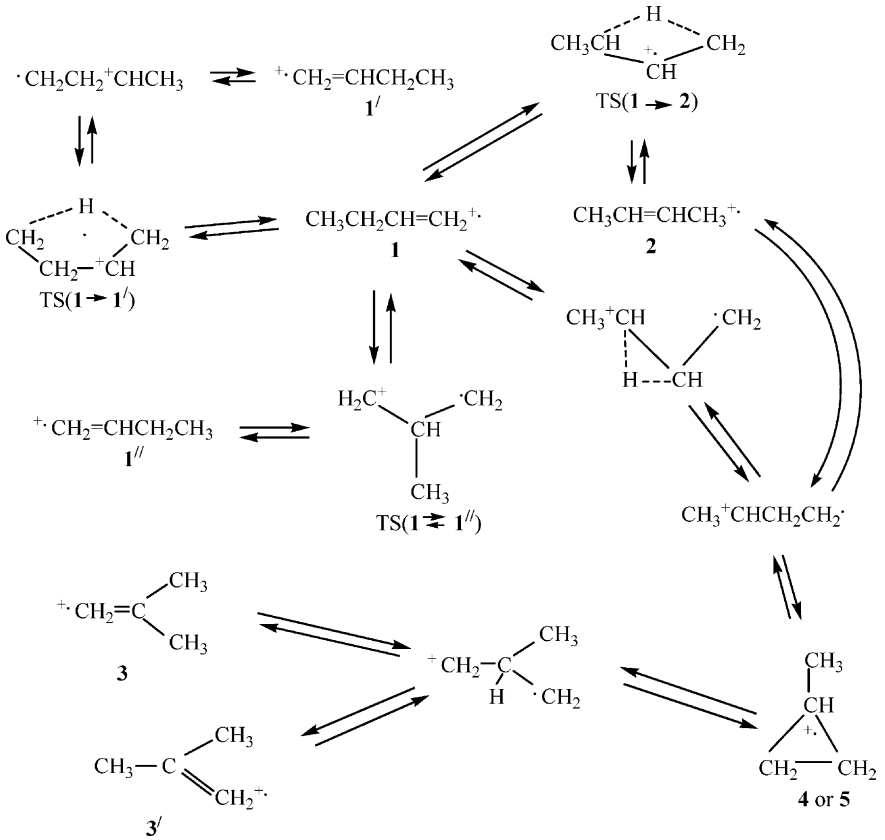

methods [17,18] utilizing B3LYP/6-31G(d,p) theory. IRC calculations employed mass weighted internal coordinates and were limited to 200 steps.

3. Results and discussion

3.1. Stable structures

Stable structures **1**–**5** are depicted in Figs. 1–5, and transition states are illustrated in association with following individual discussions of each reaction. All figures are from QCISD/6-31G(d,p) results. Energies obtained at several levels of theory are given in Tables 1 and 2. Throughout this contribution, for simplicity we will usually only quote energies from QCISD(T)/6-311G(d,p) and PMP3/6-311G(d,p) theory, although results for two lower levels of theory are available in the tables. Two stable isomers of **1** were found (Fig. 1a and b), a lower energy one with all four carbons in the same plane and a 0.3 to 4.1 kJ mol^{-1} higher energy one (**1a**) with the methyl almost perpendicular to the plane of the other three carbons. Only *trans*-**2** was characterized (Fig. 2), as we expected interconversion of that isomer with

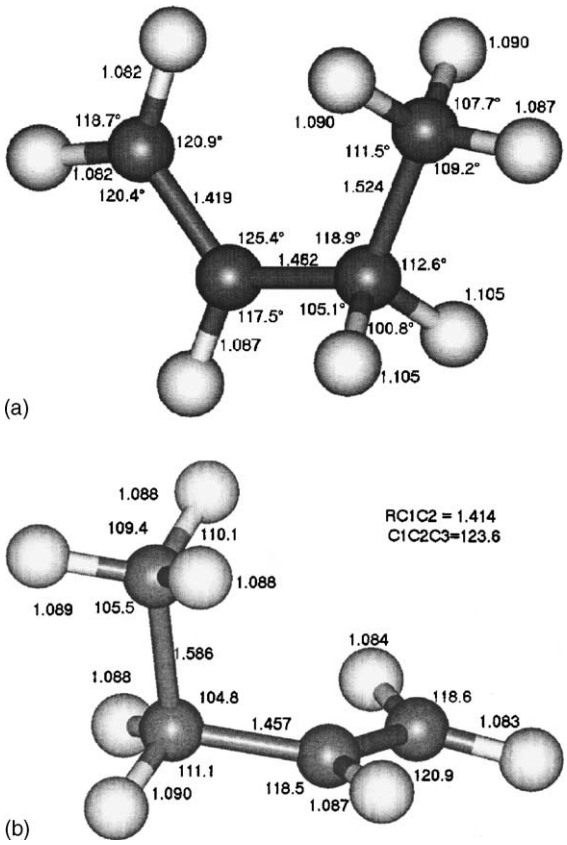

Fig. 1. (a) Geometry of the most stable configuration of the 1-butene ion (**1**) according to QCISD/6-31G(d,p) theory. In this geometry, the four carbons are in the same plane. (b) A slightly higher energy configuration of **1** in which the methyl is approximately perpendicular to the plane of the other three carbons.

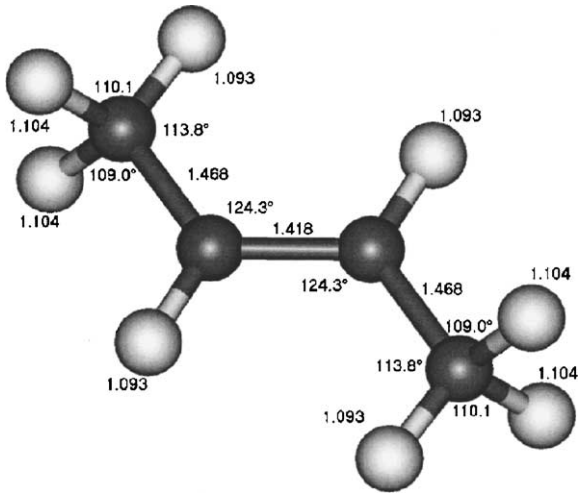

Fig. 2. Geometry of the *trans*-2-butene ion, **2**. As would be expected, the carbons and the hydrogens attached to C2 and C3 are all in the same plane.

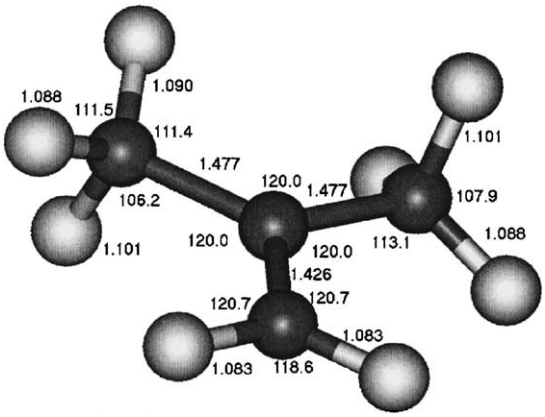

Fig. 3. The 2-methylpropene ion at its QCISD/6-31G(d,p) geometry. The hydrogens attached to C1 and all of the carbons are in the same plane.

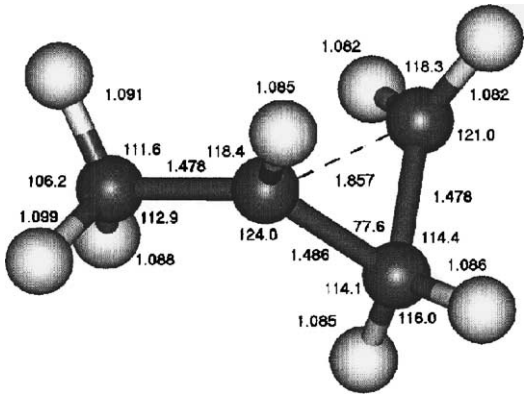

Fig. 4. The QCISD/6-31G(d,p) 1-methylcyclopropane ion. This structure is characterized by a substantially elongated RC1C3.

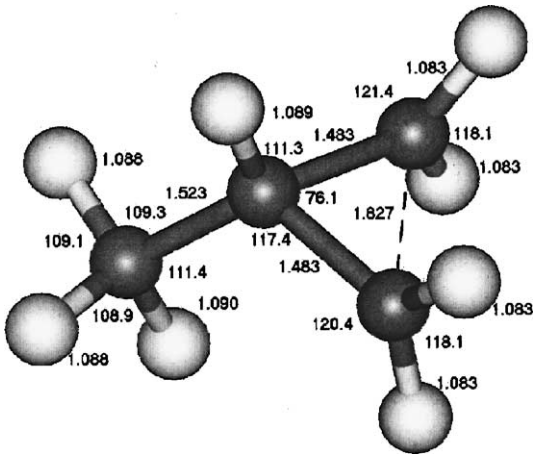

Fig. 5. The QCISD/6-31G(d,p) 2-methylcyclopropane ion. This structure is characterized by a lengthened RC2C3.

1 at lower energies than with *cis*-**2**. Structures **1**–**3** have no unusual features, and, except for **1a**, most of their structural parameters match within 0.03 Å and a few tenths of a degree those obtained previously by Eriksson and coworkers [24]. As in earlier work [25], two isomers of the methylcyclopropane radical cation, one with an elongated bond between C1 and C3 (**4**) and another with a long bond between C2 and C3 (**5**), were found (Figs. 4 and 5). Our results place **4** very close to **1** in energy, and **5** is 22 kJ mol^{-1} −24 kJ mol^{-1} above **1**. Carbons are numbered as follows in the structures to be described throughout this work; the numbering in precursors is retained throughout reactions.

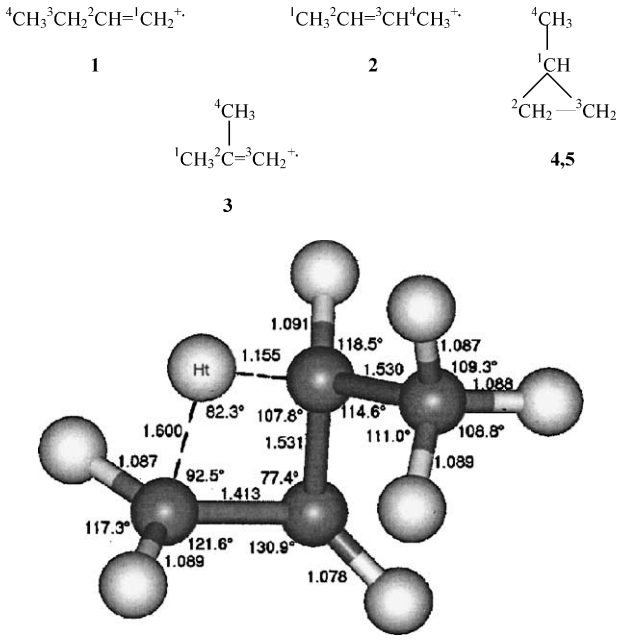

Fig. 6. The QCISD/6-31G(d,p) transition state for the interconversion of **1** and **2** by direct 1,3-H-shifts. Note that H_t is well away from C2 and closer to C1 than to C3 in this transition state. Note also that H_t approximately bisects the HCH and HCC angles of the reaction termini.

3.2. $CH_3CH_2CH{=}CH_2{}^{\bullet+}$ (*1*) → $CH_3CH{=}CHCH_3{}^{\bullet+}$ (*2*), *a 1,3-H-shift*

Paralleling the reactions of the propene radical cation [13–15], two pathways were found for **1** → **2**, one a simple 1,3-H-shift (Fig. 6), and one essentially two consecutive

Table 1
Ab initio energies (Hartrees) for $C_4H_8{}^{\bullet+}$ isomers and transition states

Species	B3LYP/6-31G(d,p)	QCISD/6-31G(d,p)	QCISD(T)/6-311G(d,p)	PMP3/6-311G(d,p)	ZPVE (kJ mol^{-1})
2-Butene$^{\bullet+}$ (**2**)	−156.920074	−156.421368	−156.486800	−156.459178	276.0
1-Butene$^{\bullet+}$ (**1**)	−156.895381	−156.400622	−156.465932	−156.438425	275.4
1-Butene$^{\bullet+}$ (**1a**)	−156.896438	−156.401464	−156.467408	−156.438850	279.6
2-Methylpropene$^{\bullet+}$ (**3**)	−156.915602	−156.419996	−156.466320	−156.458023	275.1
1-Me-cyclopropane$^{\bullet+}$ (**4**)	−156.894346	−156.400875	−156.468722	−156.440961	278.9
2-Me-cyclopropane$^{\bullet+}$ (**5**)	−156.879652	−156.389244	−156.457265	−156.429616	277.0
TS (**1** → **1′**)[a]	−156.845515	−156.342579	−156.415410	−156.384395	265.8
TS (**1** → **2s**)	−156.872758	−156.369200	−156.439526	−156.411908	268.1
TS (**1** → **2a**)	−156.839861	−156.347876	−156.418341	−156.389466	272.0
TS (**1** → **1″**)[b]	−156.852344	−156.352654	−156.422702	−156.394962	273.6
TS (**3** → **3′**)	−156.858460	−156.360473	−156.431644	−156.405134	267.4
TS (**1** → **4**)	−156.871920	−156.373037	−156.439796	−156.410859	269.4
TS (**3** → **5**)	−156.847679	−156.346210	−156.416010	−156.387571	271.4
TS (**4** → **5**)	−156.879417	−156.388687	−156.456892	−156.428982	276.1
H$^{\bullet}$	−0.498231	−0.498231	−0.499809	−0.499809	–
$CH_3CHCHCH_2{}^+$	−156.327553	−155.837349	−155.904614	−155.873253	247.6
H$^{\bullet}$ + $CH_3CHCHCH_2{}^+$	−156.825784	−156.335580	−156.404423	−156.373062	247.6
$^{\bullet}CH_3$	−39.842880	−39.713718	−39.732201	−39.726659	76.6
$CH_2CHCH_2{}^+$	−116.979592	−116.617407	−116.665936	−116.641724	176.3
$^{\bullet}CH_3$ + $CH_2CHCH_2{}^+$	−156.822472	−156.331125	−156.398137	−116.368383	252.9

[a] 1,4-H-shift.
[b] 1,3-Methyl-shift.

Table 2
Ab initio energies (kJ mol^{-1}) for $C_4H_8^{\bullet+}$ isomers and transition states

Species	B3LYP/6-31G(d,p)	QCISD/6-31G(d,p)	QCISD(T)/6-311G(d,p)	PMP3/6-311G(d,p)	Experimental values[a]
2-Butene $^{\bullet+}$ (**2**)	0	0	0	0	887
1-Butene$^{\bullet+}$ (**1**)	63.2	53.9	54.2	53.9	945
1-Butene$^{\bullet+}$ (**1a**)	65.6	55.9	54.5	57.0	–
2-Methylpropene$^{\bullet+}$ (**3**)	10.8	2.7	2.8	2.1	897
1-Methylcyclopropane$^{\bullet+}$ (**4**)	70.4	56.7	50.4	50.7	938
2-Methylcyclopropane$^{\bullet+}$ (**5**)	107.1	85.3	78.5	78.6	–
TS (**1** → **1′**)	196.7	196.7	177.2	186.1	–
TS (**1** → **2s**)	116.3	129.1	116.2	116.2	–
TS (**1** → **2a**)	119.8	120.3	116.8	120.3	–
TS (**1** → **1″**)	175.4	178.0	165.9	166.2	–
TS (**3** → **3′**)	206.6	189.0	175.7	179.0	–
TS (**1** → **4**)	153.2	151.3	136.2	133.3	–
TS (**3** → **5**)	185.5	192.7	181.3	183.4	–
TS (**4** → **5**)	106.8	85.9	78.6	79.4	–
$CH_3CHCHCH_2^+ + H^{\bullet}$	224.1	201.7	192.8	202.6	1079
$CH_2CHCH_2^+ + {}^{\bullet}CH_3$	238.2	218.8	214.7	220.3	1091

[a] 0 K values from ref. [5].

1,2-H-shifts (Fig. 7). At the 1,3-transition state, the transferring H is much closer to C3 (1.155 Å) than to C1 (1.600 Å), i.e. the transition state is nearer to the higher energy species **1**, in accord with Hammond's postulate [26]. (We will refer to the transferring hydrogen as H_t throughout, although it originates from different positions in different reactions.) Based on the IRC, H_t stays near the C1C2C3 plane in the course of this 1,3-shift, crossing this plane three times before the C2C3C1H_t dihedral angle exceeds ±2°. This angle finally goes to −10° as **2** is attained. The CH_2 departed by H_t is almost symmetrical to the C1C2C3 plane (the HC1C2C3 dihedral angles for methylene hydrogens are 93.4° and −96.2° at the transition state). Methylene is also turned to perpendicular to the skeletal plane during 1,3-H-shifts between O and C during interconversions of acetaldehyde, acetone and acetic acid radical cations with their enol isomers [21,27], so present results further indicate the generality of this type of geometry for 1,3-shifts across double bonds. C1 and C3 move toward each other as the transition state is approached and then apart after it is passed. (RC1C3 = 1.843 Å at the transition state versus 2.551 Å in **2**; throughout this text, R = the distance between two accompanying atoms.) However, there is essentially no bonding between C1 and C3 at the transition state. (The QCISD/6-31G(d,p) overlap population between C1 and C3 equals −0.118).

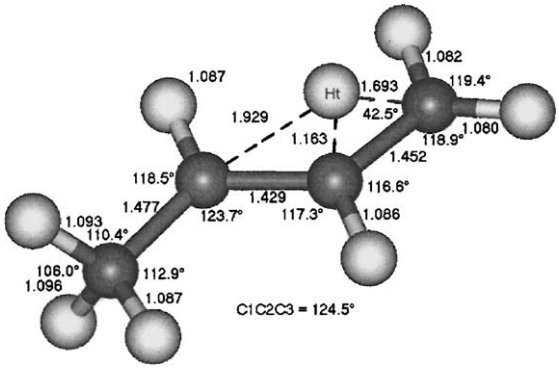

Fig. 7. The QCISD/6-31G(d,p) transition state for interconverting **1** and **2** by two consecutive 1,2-H-shifts. Note that H_t is bonded to C2 at this point, even though this structure is not at a potential minimum.

In two stage **1** → **2**, H_t first moves from C3 to close to C2 and then to C1. At the closest approach of H_t to C2, 1.148 Å according to the IRC from B3LYP/6-31G(d,p) theory, RC2H_t is close to a normal CH bond length. A B3LYP/6-31G(d,p) result is given because it was taken from an IRC trace obtained at that level of theory. This point is near but not at the transition state. At the QCISD/6-31G(d,p) TS (**1** → **2**), the overlap populations between H_t and C1, C2 and C3 are 0.028, 0.538 and −0.0393, respectively, demonstrating predominant bonding to of H_t to C2 at that point. Thus, paralleling $C_3H_6^{\bullet+}$ reactions [14,15], this reaction is effectively two consecutive 1,2-H-shifts separated at $CH_3^+CHCH_2CH_2^{\bullet}$, even though this is a transition state rather than a stable intermediate. At this transition state, H_t is closer to C1 (1.693 Å) than to C3 (1.929 Å), i.e. the transition state is closer to **2** than to **1**, contrary to Hammond's postulate. We will discuss this feature further below. H_t is well above the C1C2C3 plane throughout its migration, with the H_tC1C2C3 dihedral angle being 89.9° at the transition state, making the reaction suprafacial. However, even if it is suprafacial, since it effectively occurs in two steps, it is not restrained by conservation of orbital symmetry, as would be a direct 1,3-suprafacial H-transfer [21,28].

The transition states for both **1** → **2** isomerizations are well below the lowest energy $C_4H_8^{\bullet+}$ dissociations [5], so these are important $C_4H_8^{\bullet+}$ reactions. The transition state energies for the two pathways are within 10 kJ mol^{-1} of each other at all four levels of theory applied, that is, within the uncertainty of the calculations. The similarity in the critical energies for 1,2- and 1,3-H-shifts contrasts markedly with

the situation in $C_nH_{2n}O^{\bullet+}$ systems in which 1,2-H-shifts have moderate critical energies [29–31] and 1,3-H-shifts have high critical energies [21,32].

3.3. $CH_3CH_2CH{=}CH_2^{\bullet+}$ (1) → $CH_2{=}CHCH_2CH_3^{\bullet+}$ (1′), consecutive 1,4- and 1,2-H-shifts

We found two degenerate isomerizations of **1** by H-transfers. One of them, the consecutive 1,4-H – 1,2-H-shifts (**1** → **1′**), also traverses a $CH_3{}^+CHCH_2CH_2^{\bullet}$ structure, this time between the 1,4-H- and 1,2-H-shift stages. Again, this point is not a potential energy minimum, but it differs in geometry from TS (**1** → **2**). In **1** → **1′**, H_t is first transferred between C1 and C4. At the transition state (Fig. 8), which occurs during the 1,4-H-shift, H_t is closer to its destination (C1, 1.289 Å) than to its origin (C4, 1.503 Å), but H_m, the hydrogen that migrates from C3 to C2 in the second stage of this reaction, is not yet moving significantly (RH_mC = 1.098 Å). At TS (**1** → **1′**) the C2 and C4 methylenes are approximately bisected by the plane containing C1, C4 and H_t, while the C1 methylene is somewhat angled relative to that plane (Fig. 8b). Since **1** is both the reactant and the product, the stages can also take place in the reverse order.

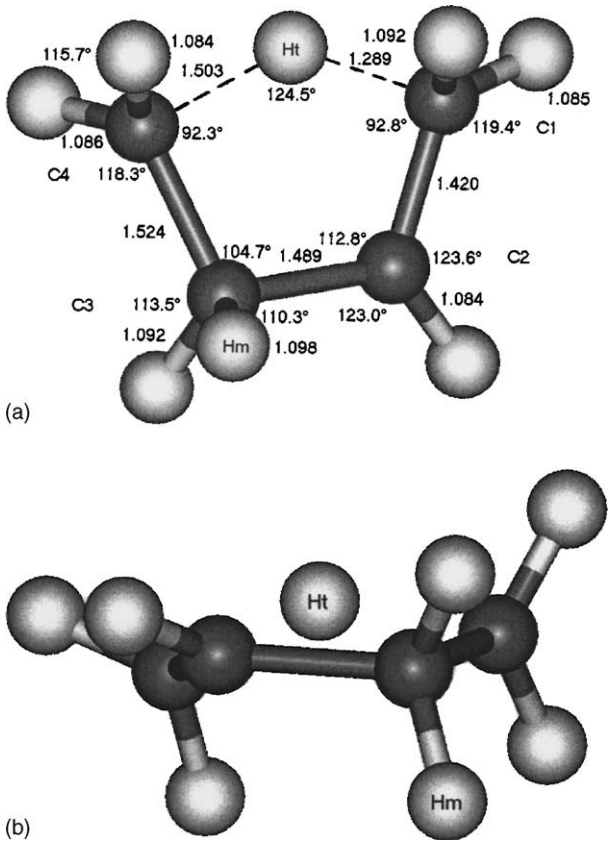

Fig. 8. The transition state (QCISD/6-31G(d,p) theory) for the degenerate isomerization **1** → **1′**. (a) Facial view. Note that H_t is closer to C1 than to C4, and that the hydrogen (H_m) on C3 that will migrate to C2 has not yet begun to move. (b) Edge on view of TS (**1** → **1′**) showing orientations of CH bonds relative to the approximate CCCC plane. HC1H is somewhat rotated relative to the approximate CCCC plane, and HC3H and HC4H are approximately perpendicular to that plane.

In the second stage of **1** → **1′**, pathway tracing shows that the H_m C3C2C1 dihedral angle changed from 124° to 89.5°, i.e. H_m passes above the C3C2 axis when H_m is approximately half transferred. At this point, the four carbons are nearly planar (C4C3C2C1 dihedral angle = −7°), and the hydrogens on C1 and C2 are nearly in this plane. When H_m is close to half transferred, the two hydrogens on C4 are also both near the skeletal plane (dihedral angle H1C4C3C2 = −12.5° and H2C4C3C2 = 169.2°. The hydrogens on C1 and C2 move toward or away from the skeletal plane as H_m moves from and to the carbon on which they reside. Most likely the overall reaction occurs in two stages because it is impossible to accommodate the disparate geometries required for the 1,4-and 1,2-shifts in the same structure. This contrasts with 1,2-H-shifts that in concert with bond-breakings form secondary rather than primary carbocations [33–37], presumably because the geometries of those transition states provide no impediments to concerted processes.

TS (**1** → **1′**) is 61–70 kJ mol^{-1} higher in energy than TS (**1** → **2**). This is rather surprising because in most radical cations 5-membered ring H-transfers are substantially lower in energy than 4-membered ring H-transfers [38,39]. The energy at TS (**1** → **1′**) is below the dissociation thresholds, so this reaction should contribute to the H-reshuffling that precedes $C_4H_8^{\bullet+}$ dissociations.

3.4. $CH_3CH_2CH{=}CH_2^{\bullet+}$ (1) → $CH_2{=}CHCH_2CH_3^{\bullet+}$ (1″), a 1,3-methyl-shift

A transition state for another degenerate isomerization of **1**, the 1,3-methyl shift **1** → **1″**, was also found (Fig. 9).

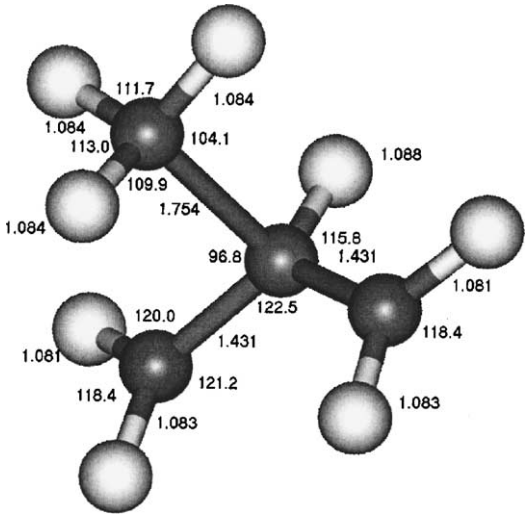

Fig. 9. The QCISD/6-31G(d,p) transition state for the 1,3-methyl shift **1** → **1″**. The methyl carbon is halfway between C1 and C3 (see text) and above C2 relative to the C1C2C3 plane.

The IRC calculation shows that during **1** → **1″**, RC1C4 steadily decreases and RC3C4 simultaneously increases. All of the following parameters for **1** → **1′** are from QCISD/6-31G(d,p) theory. At TS (**1** → **1″**), the itinerant methyl is located symmetrically between C3 and C1 (Fig. 9). The moving methyl is much closer to C2 (1.754 Å) at the transition state than to the migration termini (2.392 Å), suggesting that, as in suprafacial 1,3-H-shifts characterized in this work, there is substantial methyl–C2 bonding at this point. Overlap populations between the migrating methyl carbon and C1, C2 and C3 of −0.028, 0.534 and −0.028 confirm this, demonstrating that there is bonding only between the methyl carbon and C2. Charge and spin are equally concentrated on C1 and C3 at the transition state: charge densities summed to heavy atoms are 0.330 and 0.330, corresponding spin densities without such summing are 0.683 and 0.683. Similar distributions were found for the other branched transition states, so for these there are not separated charge and radical sites. The HCCC dihedral angles for the hydrogens on C1 and C3 range from −13.7° to 173.4°, i.e. nearly flat, so at the transition state C_3H_5 approximates an allyl structure (Fig. 9). The C4C3C2C1 dihedral angle traced by the IRC starts at −85.4° and reaches −107.7° after the transition state, which starts and ends at **1a** in our IRC. The migrating methyl stays on the same side of the plane of the other three carbons throughout the reaction. At the transition state, the methyl carbon is equidistant from H6 and H8 (2.884 and 2.885 Å), H5 and H9 (2.949 and 2.946 Å) and C1 and C3 (2.398 and 2.392 Å). (H6 and H8 are on C1 and C3 respectively and *cis* to the hydrogen on the middle carbon; H5 and H9 are correspondingly trans.) Thus, the methyl carbon is approximately above the middle carbon at this transition state (Table 3).

The threshold for **1** → **1″** is above those for 1,2- and 1,3-H-transfers, below that for five-membered ring **1** → **1′** and substantially below those for the lowest energy $C_4H_8^{\bullet+}$ dissociations (Tables 1 and 2). Thus, this reaction should contribute to the redistributions of carbons and hydrogens that accompany the decompositions of $C_4H_8^{\bullet+}$.

Table 3
Charge and spin densities in branch-chain transition states based on QCISD/6-31G(d,p) theory

Structure		C1	C2	C3
TS (1 → 1″)	C[a]	0.330	−0.006	0.330
	S	0.683	−0.138	0.684
TS (3 → 3′)	C[a]	0.311	0.156	0.311
	S	0.677	−0.149	0.677
TS (5 → 3)	C[a]	0.416	0.0009	0.367
	S	0.527	−0.093	0.694

[a] Charges on hydrogen atoms summed to the carbon to which they are attached.

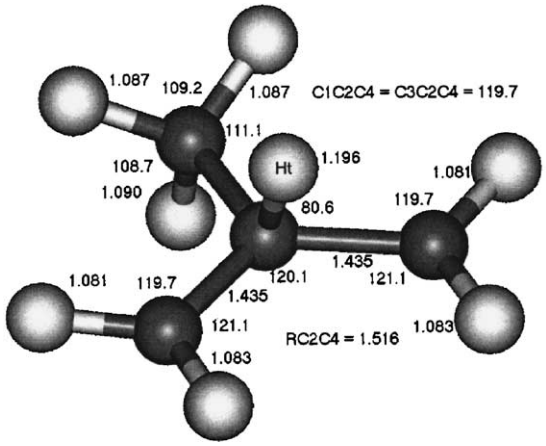

Fig. 10. The QCISD/6-31G(d,p) transition state for the 1,3-H-shift **3** → **3′**. Note that the four carbons and the hydrogens attached to C1 and C3 are roughly planar, and that H_t is almost a normal bond length from C2. H_t is directly above a point on the skeletal plane between a line between C1 and C3 and the location of C2. The reaction occurs essentially by two consecutive 1,2-H-shifts.

3.5. $CH_3C(CH_3)=CH_2^{\bullet+}$ (3) → $CH_2=C(CH_3)CH_3^{\bullet+}$ (3′), another 1,3-H-shift

We also located a transition state for **3** → **3′**, a degenerate isomerization of the 2-methylpropene ion by a 1,3-H-shift (Fig. 10). At the suprafacial transition state, all of the carbons and hydrogens attached to C1 and C3 are close to being in the same plane, forming another allyl-like unit. The IRC calculation shows that H_t stays above this plane throughout the course of the reaction and is approximately over C2 at the transition state. H_t is symmetrical to C1 and C3 (1.712 Å from each carbon) and to the hydrogens on those carbons *cis* (2.757 Å) and trans (3.546 Å) to the methyl at the transition state. As in **1** → **2** and the methyl shift in **1** → **1″**, H_t develops substantial bonding while passing the middle carbon (distance at the TS = 1.196 Å and overlap populations between H_t and C1, C2 and C3 = −0.006, 0.514 and –0.006). This transition state is about 60 kJ mol^{-1} higher in energy than that for the suprafacial 1,3-H-shift **1** → **2**. The higher energy of this transition state is probably due to concentration of charge at primary sites in TS (**3** → **3′**) versus a secondary site in $CH_3^+CHCH_2CH_2^{\bullet}$. A 1,3-H-shift transition state for **3** → **3′** was sought, but not found.

3.6. 1-Methylcyclopropane cation (4) → $CH_3CH_2CH=CH_2^{\bullet+}$ (1), a ring opening—1,2-H-shift

This pathway is analogous to that for the cyclopropane–propene radical cation interconversion found by Borden and coworkers [15]. The ring of the methylcyclopropane cation with a long bond between C1 and C2 (**4**) opens by further extension of that bond (Fig. 11). As in **1** → **1′**, formation of the distonic structure, in this case by ring opening, largely precedes the transition state, and H-transfer occurs after the transition states. Between **4** and the transition state,

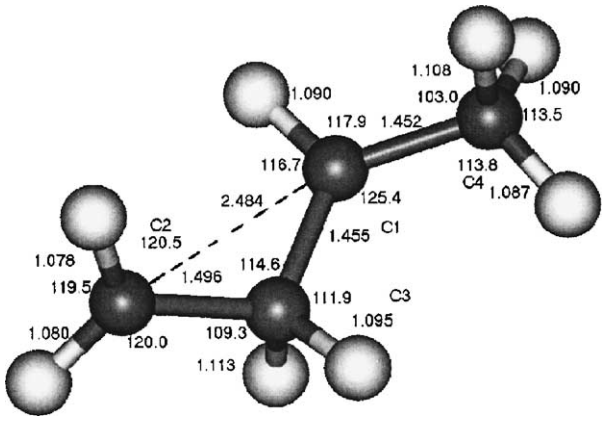

Fig. 11. The transition state for the ring opening **4** → **1**, QCISD/6-31G(d,p) theory. Note the migration of H_t from C3 to C1 that will complete the reaction is not yet significant. Also, the C3 methylene is still almost perpendicular to the C1C3C2 plane, but the C2 methylene has rotated substantially relative to its orientation in the ring.

RC1C3 elongates from 1.857 Å to 2.484 Å, approaching its distance in **1**, 2.560 Å. RC3H_t increases from 1.086 Å at **4** to 1.113 Å at the transition state to 3.253 Å at **1**. Again, $CH_3^+CHCH_2CH_2^\bullet$ is not a potential energy minimum.

Even though there are paths to it from **1**, **2** and **4**, we never found a $CH_3^+CHCH_2CH_2^\bullet$ energy minimum. Except for a 1,2-shift going from **1** to the distonic structure, a shift that does not have a transition state, each of these pathways passes through a transition state with a substantially different $CH_3^+CHCH_2CH_2^\bullet$ structure, reflecting the different locations and energies of the barriers they have to cross from their points of origin.

The energy for TS (**4** → **1**), 133–136 kJ mol^{-1}, is lower than that for any of the other reactions except **1** → **2** and **4** → **5**. Given that the energy of TS (**1** → **4**) is 57 – 69 kJ mol^{-1} below the threshold for $H^\bullet$ loss, interconversion of **1** and **4** undoubtedly occurs below the onsets of dissociation.

3.7. Why do reaction pathways go to *1* rather than *2*?

It is noteworthy and perhaps surprising that the minimum energy pathways through $CH_3^+CHCH_2CH_2^\bullet$ from both **1** and **4** lead to higher energy **1** rather than to lower energy **2**. This may result from the distributions of charge and spin densities in $CH_3^+CHCH_2CH_2^\bullet$. Barriers for 1,2-shifts are very high in energy in alkyl radicals [29,40,41], intermediate for radical cations [28–30], and negligible for primary to secondary 1,2-H-shifts in carbocations [42]. At the distonic point in **4** → **1**, the Mulliken charges on carbons C2, C3, C1 and C4 are respectively −0.200, −0.328, 0.157 and −0.417 (numbering as for **4**). Three of these values are negative, and together they sum to far less than +1.00 because the Mulliken analysis allocates substantial positive charge to hydrogens. However, C1 is the most positively charged in this treatment, i.e. has the most carbocation character. Spin densities allocated to the heavy atoms in the same order are 1.071, −0.086, 0.104 and −0.003. Thus, the radical site resides largely on the terminal carbon, and C1 carries the most positive charge. This distribution may cause the reaction to proceed from $CH_3^+CHCH_2CH_2^\bullet$ to higher energy **1** rather than directly to the more stable **2**.

Table 4
Transition state parameters for reactions that pass through $CH_3^+CHCH_2CH_2^\bullet$

Transition state	E (kJ mol^{-1})	RH_tC1 (Å)	RH_tC3 (Å)
TS (**1** → **2s**)	129.1	1.693	1.929
1 → **1′**[a]	55.7	2.129	2.055
TS (**4** → **1**)	151.3	2.140	1.977

[a] For the point where the B3LYP/6-31G(d,p) IRC stopped for **1** → **1′**, a $CH_3^+CHCH_2CH_2^\bullet$ structure, but not a transition state. Further tracing of the pathway from this point led to **1′**. All other parameters are from QCISD/6-31G(d,p) theory.

However, $CH_3^+CHCH_2CH_2^\bullet$ would not be expected to have a strong bias to go to **1** rather than **2** because **1** → **2** through that structure is the lowest energy H-transfer that we found (Table 2). Since the transition state energies for **1** → **1′** and **4** → **1** are higher than that for **1** → **2**, reactions starting out on those pathways should also be able to branch to **2**. We attribute the IRCs going to **1** rather than to **2** to TS (**1** → **1′**) and TS (**4** → **1**) being closer to the geometry of **1** than of **2** (see Table 4), i.e. those pathways go down the side of the TS (**1** → **2**) barrier toward **1**. Based on the relative transition state energies, it is likely that in reality **1** and **4** isomerize directly to **2** as well as to **1** because after transiting their transition states they would contain enough energy to travel above the minimum energy pathway.

3.8. 1-Methylcyclopropane cation (*4*) → 2-methylcyclopropane cation (*5*)

In **4** → **5**, the elongated RC2C3 simply shortens and RC1C3 lengthens until isomerization is complete. The transition state for this reaction is pictured in Fig. 12. At a

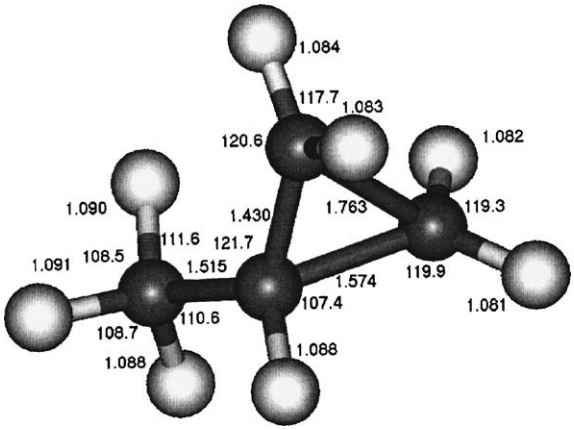

Fig. 12. Transition state for the interconversion of the methylcyclopropane isomers. Note that in this transition state RC2C3 is shorter and RC1C2 is longer than in the 2-methylcyclopropane ion (Fig. 5).

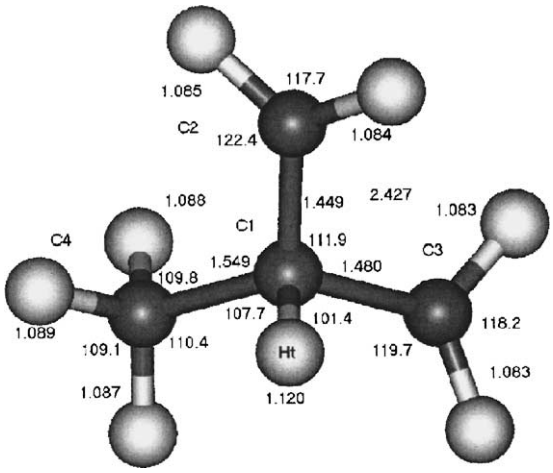

Fig. 13. The QCISD/6-31G(d,p) transition state for the ring opening **2** → **5** by elongation of RC2C3. Note that H_t has not moved toward C2 at this point.

critical energy of 79 kJ mol^{-1} (Table 2), **4** → **5** is the lowest energy $C_4H_8^{\bullet+}$ isomerization. Redistribution of carbon atoms in the $C_4H_8^{\bullet+}$ system likely occurs primarily by **1** → **4** → **5** → **4** → **1**, as the critical energies for **1** → **4** and **4** → **5** are both below that for the other $C_4H_8^{\bullet+}$ skeletal rearrangement, **3** → **3′**.

3.9. 2-Methylcyclopropane cation (5) → $CH_3C(CH_3)=CH_2^{\bullet+}$ (3), another ring opening—1,2-H-shift

Similarly to **4** → **1**, in **5** → **3** a long C2–C3 bond opens and then an H shifts, this time from C1 to C2 to form **3**. At the transition state for this reaction, the breaking CC bond is lengthened from 1.827 Å (Fig. 5) to 2.427 Å while the CH_t bond, at 1.120 Å (versus 1.089 Å in **5**), has scarcely begun to lengthen (Fig. 13). This $^{\bullet}CH_2CH(CH_3)CH_2^{\bullet+}$ also is not at an energy minimum. Thus, as in **1** → **1′** and **3** → **3′**, in **4** → **1** and **5** → **3** ring opening/closing and H-shifting are distinct stages rather than steps in the reaction. For the H-shift in **5** → **3** to occur, the C2C3 bond has to break and the CH_2 to which the H is transferred rotates from being symmetrically bisected by the plane of the ring carbons to being nearly in that plane. H_t essentially begins to transfer from C1 only when the methylene is nearly in the CCC plane. (The HC2C1C3 dihedral angles are 91.8° and −91.9° at **5**, 175.1° and −13.1° at the point at which RCH has increased by 0.1 Å, 173.5° and 0.5° when RCH_t is 1.455 Å and the CH_2 closest to being in the skeletal plane, and at 151.6° and 23.5° in the newly formed methyl.)

Energetically, TS (**5** → **3**) is 50-55 kJ mol^{-1} higher than TS (**4** → **1**), so the former reaction is probably less frequent than the latter. However, **5** → **3** probably does occur, since its threshold is 12 – 19 kJ mol^{-1} below that for $H^{\bullet}$ loss, the lowest threshold dissociation of $C_4H_8^{\bullet+}$ [5].

Although still distinct, the transition states for the pathways leading through $^{\bullet}CH_2CH(CH_3)CH_2^{+}$, **1** → **1″**, **3** → **3′** and **5** → **3** are more similar (Figs. 9, 10 and 13) than the transition states on different pathways through $CH_3^{+}CHCH_2CH_2^{\bullet}$. The transition state for methane elimination from the 1-butene ion also resembles the present branched transition states [43]. For comparison of the geometries of those transition states, pertinent structural parameters of the former are given in Table 5. Corresponding parameters for transition states for hydrogen versus methyl transfer are quite similar, except in one case the methyl is moving above the approximate plane of most of the rest of the ion and in the other case the H atom is so moving. As for H_t, this brings the methyl closer to H6 and H8 at the transition state for its migration versus when it is stationary on C2. Bond lengths in the transition state for ring opening/closing are rather similar to those in TS (**1** → **1″**) and TS (**3** → **3′**), but the CH_2 groups are much more twisted relative to the skeletal plane in TS (**5** → **3**), reflecting that they have rotated, but not yet completely into the skeletal plane at this transition state.

Table 5
Structural parameters for branched chain transition states

Parameter	**3** → **3′** 1,3-H-shift	**1** → **1″** 1,3-Me-shift	**5** → **3** Ring opening
RC1C2	1.435	1.431	1.449
RC2C3	1.435	1.431	1.480
RC2C4	1.516	1.754	1.549
RC1C3	2.488	2.509	2.427
RC1C4	2.553	2.393	2.557
RC3C4	2.553	2.392	2.552
RC2H5	1.186	1.088	1.120
RC1H5	1.712	2.142	2.002
RC3H5	1.711	2.143	2.025
RC4H6	3.546	2.949	3.554
RC4H7	2.757	2.884	2.774
RC4H8	3.546	2.946	3.304
RC4H9	2.757	2.885	3.084
Angles			
C1C2C3	120.1	122.5	111.9
H5C2C4	115	101	108
H5C2C3	83.5	115.8	101.7
Dihedral angles			
H6C1C2C3	2.5	13.4	−46.0
H7C1C2C3	−184.0	−173.6	132.6
H8C3C2C1	−2.5	173.4	−28.4
H9C3C2C1	−175.9	−13.7	143.4

3.10. $CH_3CH_2CH_2CH=CH_2^{\bullet+}$ (6) → $^{\bullet}CH_2CH_2CH_2^{+}CHCH_3$ (7)

Six-membered ring transfers (1,5-shifts) are perhaps the most prominent isomerizations in gas phase ion chemistry [44]. Since they cannot occur in $C_4H_8^{\bullet+}$ ions, we characterized the 1,5-H-shift in the 1-pentene ion (Figs. 14 and 15), i.e. the first step of the McLafferty rearrangement, to compare a 1,5-H-shift and the $C_4H_8^{\bullet+}$ rearrangements. The size of the 1-pentene ion and the complexity of the $C_5H_{10}^{\bullet+}$ potential surface made it impractical to treat $C_5H_{10}^{\bullet+}$ reactions

Table 6
Ab initio energies (Hartrees) for the McLafferty rearrangement of $CH_3CH_2CH_2CH{=}CH_2^{\bullet+}$

Species	B3LYP/6-31G(d,p)	QCISD/6-31G(d)	QCISD (T)/6-311G(d,p)	PMP3/6-311G (d,p)	ZPVE (kJ mol^{-1})
$CH_3(CH_2)_2CH{=}CH_2^{\bullet+}$ (**6**)	−196.217516	−195.519704	−195.684072	−195.646932	353.5
$CH_3(CH_2)_2CH{=}CH_2^{\bullet+}$ (**6a**)	−196.213945	−195.517551	−195.680970	−195.645295	350.6
$CH_2CH_2CH_2CH^+CH_3$ (**7**)	−196.203554	−195.501089	−195.667397	−195.629151	348.9
TS (**6** → **7**)	−196.199972	−195.494961	−195.666006	−195.629775	347.3
$CH_2{=}CH_2$	−78.593808	−78.313352	−78.384226	−78.367386	134.2
$CH_3CH{=}CH_2^{\bullet+}$	−117.573840	−117.157311	−117.249421	−117.229465	201.0

Table 7
Ab initio energies (kJ mol^{-1}) for the McLafferty rearrangement of $CH_3CH_2CH_2CH{=}CH_2^{\bullet+}$

Species	B3LYP/6-31G(d,p)	QCISD/6-31G(d)	QCISD(T)/6-311G(d,p)	PMP3/6-311G(d,p)
$CH_3(CH_2)_2CH{=}CH_2^{\bullet+}$ (**6**)	0	0	0	0
$CH_3(CH_2)_2CH{=}CH_2^{\bullet+}$ (**6a**)	6.4	2.8	5.2	1.4
$^{\bullet}CH_2CH_2CH_2CH^+CH_3$ (**7**)	32.0	44.3	39.2	42.1
TS (**6** → **7**)	39.9	58.8	41.2	38.8
$CH_2{=}CH_2 + CH_3CH{=}CH_2^{\bullet+}$	112.6	110.5	114.1	113.2

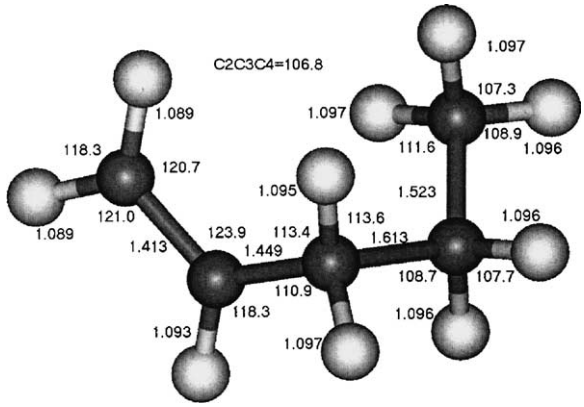

Fig. 14. The QCISD/6-31G(d,p) structure for the lowest energy isomer of the 1-pentene ion.

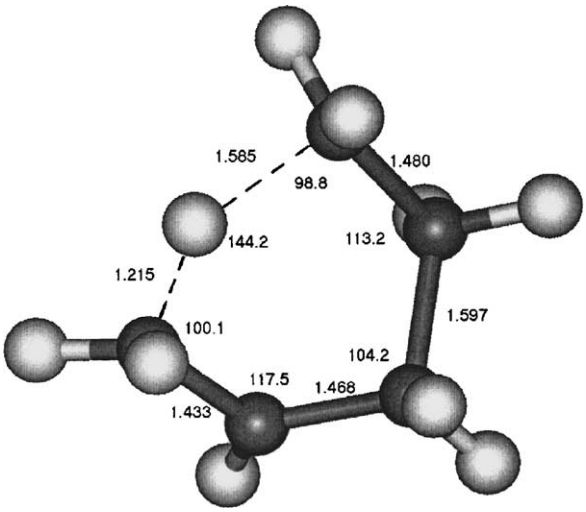

Fig. 15. The QCISD/6-31G(d,p) transition state for 1,5-H-transfer in the 1-pentene ion. Note that H_t is moving to and from the faces of the methylene reaction termini.

as comprehensively as we have those of the $C_4H_8^{\bullet+}$ ions. Energies are given in Tables 6 and 7. Two forms of **6** quite close in energy and similar in structure were found. Our results place the distonic intermediate $^{\bullet}CH_2CH_2CH_2C^+HCH_3$ (**7**) at an energy minimum (Fig. 16). However, at our two highest levels of theory **7** requires only –0.4 to 5 kJ mol^{-1} to return to **6**, so whether **7** is at an energy minimum is not certain. As in **1** → **1′**, in TS (**6** → **7**) H_t is closer to the carbon it is approaching (1.215 Å) than to the one it is departing (1.585 Å).

The critical energy obtained for **6** → **7** is 36–37 kJ mol^{-1}. However, the dissociated products are 109–112 kJ mol^{-1} above **6**, at or very close to the energy required for 1,3-H-shifts and cyclizations in $C_4H_8^{\bullet+}$ reactions. Thus, the threshold for this 1,5-H-shift is below the energy for subsequent dissociation and any other $C_4H_8^{\bullet+}$ reaction. Therefore, six-membered ring H-transfer should be an important $C_nH_{2n}^{\bullet+}$ reaction when n > 4. However, Millard

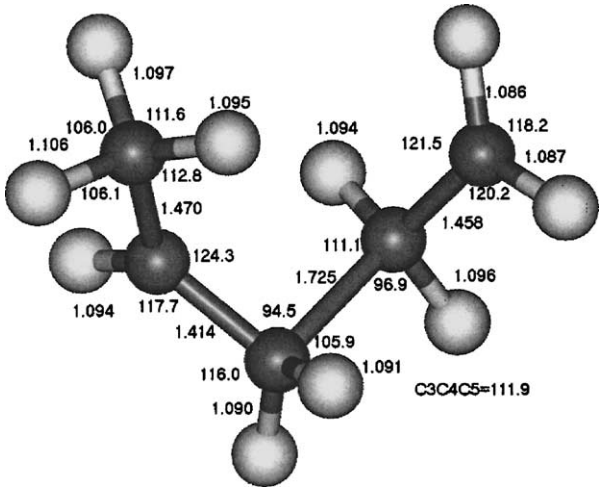

Fig. 16. The distonic product of a 1,5-H-shift by the 1-pentene ion.

and Shaw provided very good evidence for a greater importance of 1,2-H-shifts [11]. As they proposed, the latter reactions are probably entropically favored, depleting the 1-pentene ion more rapidly than the 1,5-H-transfer takes place at and above the dissociation threshold.

4. Summary

Present work systematically characterized the rearrangements that take place below the threshold for dissociation of $C_4H_8^{\bullet+}$ ions. The most common reactions are 1,3-shifts and hydrogen transfers by consecutive 1,2-H-shifts. Given that these reactions have low critical energies and also take place in $C_3H_6^{\bullet+}$, they probably occur widely in $C_nH_{2n}^{\bullet+}$ reactions. In the 1,3-H-shifts, H is transferred approximately in the skeletal plane, whereas in consecutive 1,2-shifts H-motion is approximately perpendicular to the skeletal plane. In each case the migrating group goes approximately between the atoms bonded to the destination carbon, but in one case sigma bonding places these bonds approximately perpendicular to the skeletal plane and in the other case π-bonding at allyl-like transition states puts those bonds near the skeletal plane. These geometries cause the migrating entity to move close to the skeletal plane or nearly perpendicular to it. Of particular interest is that, although 1,2-H-shifts and their tandem reactions in $C_4H_8^{\bullet+}$ occur in separate stages, those stages are separated by virtual intermediates (points that reactions pass through corresponding to a conventional structure but lacking a corresponding potential minimum) rather than by energy minima. This separation stems from differing geometric requirements for the successive stages of the reactions. The virtual intermediates and the pathways through them for different reactions to the same product are each distinct according to theory, demonstrating different minimum energy pathways traversing nearby regions of the same potential surface. A variety of reactions with virtual intermediates occur in cations in the gas phase [15,19,20,22], demonstrating that such reactions should be added to the recognized categories of isomerizations of cations in the gas phase. Critical energies for H-transfers decrease in the order 1,4 > 1,3 ≅ 1,2 > 1,5 in the $C_nH_{2n}^{\bullet+}$ ions examined, differing from the order 1,3 > 1,4 > 1,2 > 1,5 in other homologous series of aliphatic radical cations.

Acknowledgements

We thank Jason Dunsmore and Debbie Pavlu for help in preparing the manuscript.

References

[1] T. Baer, D. Smith, B.P. Tsai, A.S. Warner, Adv. Mass Spectrom. A 7 (1978) 56.
[2] W.J. Chesnavich, L. Bass, T. Su, M.T. Bowers, J. Chem. Phys. 74 (1981) 2228.
[3] G.G. Meisels, G.M.L. Verboom, M.J. Weiss, T. Hsieh, J. Am. Chem. Soc. 101 (1979) 7189.
[4] M.T. Bowers, M.F. Jarrold, W. Wagner-Redeker, P.R. Kemper, L.M. Bass, Faraday Discuss. Chem. Soc. 75 (1983) 57.
[5] J.A. Booze, M. Schweinsberg, T. Baer, J. Chem. Phys. 99 (1993) 4441.
[6] T. Nishishita, F.M. Bockhoff, F.W. McLafferty, Org. Mass Spectrom. 12 (1977) 16.
[7] G.A. Smith, D.H. Williams, J. Chem. Soc. B (1976) 1529.
[8] M.S.-H. Lin, A.G. Harrison, Can. J. Chem. 52 (1974) 1813.
[9] G.G. Meisels, J.Y. Park, B.G. Giessner, J. Am. Chem. Soc. 91 (1969) 1555.
[10] T. Hsieh, J.P. Gillman, M.J. Weiss, G.G. Meisels, J. Phys. Chem. 85 (1981) 2722.
[11] W.H. McFadden, J. Am. Chem. Soc. 67 (1963) 1074.
[12] B.J. Millard, D.F. Shaw, J. Chem. Soc. B (1966) 664.
[13] M.T. Nguyen, L. Landuyt, L.G. Vanquickenborne, Chem. Phys. Lett. 182 (1991) 225.
[14] T. Clark, J. Am. Chem. Soc. 109 (1987) 6838.
[15] P. Du, D.A. Hrovat, W.T. Borden, J. Am. Chem. Soc. 110 (1988) 3405.
[16] P. Jungwirth, T. Bally, J. Am. Chem. Soc. 115 (1993) 5783.
[17] C. Gonzalez, H.B. Schlegel, J. Chem. Phys. 90 (1989) 2154.
[18] C. Gonzalez, H.B. Schlegel, J. Phys. Chem. 94 (1990) 5523.
[19] C.E. Hudson, L. DeLeon, D. Van Alstyne, D.J. McAdoo, J. Am. Soc. Mass Spectrom. 5 (1994) 1102.
[20] C.E. Hudson, D.J. McAdoo, J. Am. Soc. Mass Spectrom. 9 (1998) 138.
[21] C.E. Hudson, D.J. McAdoo, J. Am. Soc. Mass Spectrom. 15 (2004) 972.
[22] C.E. Hudson, D.J. McAdoo, Int. J. Mass Spectrom. 232 (2004) 17.
[23] M.J. Frisch, G.W. Trucks, H.B. Schlegel, G.E. Scuseria, M.A. Robb, J.R. Cheeseman, V.G. Zakrzewski, J.A. Montgomergy Jr., R.E. Stratmann, J.C. Burant, S. Dapprich, J.M. Millam, A.D. Daniels, K.N. Kudin, M.C. Strain, O. Farkus, J. Tomasi, V. Barone, M. Cossi, R. Cammi, B. Mennucci, C. Pomelli, C. Adamo, S. Clifford, J. Ochterski, G.A. Petersson, P.Y. Ayala, Q. Cui, K. Morokuma, D.K. Malick, A.D. Rabuck, K. Raghavachari, J.B. Foresman, J. Cioslowski, J.V. Ortiz, A.G. Baboul, B.B. Stefanov, G. Liu, A. Liashenko, P. Piskorz, I. Komaromi, R. Gomperts, R.L. Martin, D.J. Fox, T. Keith, M.A. Al-Laham, C.Y. Peng, A. Nanayakkara, M. Challacombe, P.M.W. Gill, B. Johnson, W. Chen, M.W. Wong, J.L. Andres, C. Gonzalez, M. Head-Gordon, E.S. Replogle, J.A. Pople, Gaussian Int., Pittsburgh, PA, 1998.
[24] L.A. Eriksson, S. Lunell, R.J. Boyd, J. Am. Chem. Soc. 115 (1993) 6896.
[25] K. Krough-Jespersen, H.D. Roth, J. Am. Chem. Soc. 114 (1992) 8388.
[26] G.S. Hammond, J. Am. Chem. Soc. 77 (1955) 334.
[27] C.E. Hudson, D.J. McAdoo, Int. J. Mass Spectrom. 219 (2002) 295.
[28] R.B. Woodward, R. Hoffmann, Angew. Chem. Int. Ed. 8 (1969) 781.
[29] C.E. Hudson, D.J. McAdoo, Tetrahedron 46 (1990) 331.
[30] G. Bouchoux, A. Luna, J. Tortajada, Int. J. Mass Spectrom. Ion Process. 167–168 (1997) 353.
[31] C.E. Hudson, D.J. McAdoo, Int. J. Mass Spectrom. 210–211 (2001) 417.
[32] D.J. McAdoo, Mass Spectrom. Rev. 19 (2000) 38.
[33] T. Takeuchi, M. Yamamoto, K. Nishimoto, H. Tanaka, K. Hirota, Int. J. Mass Spectrom. Ion Phys. 52 (1983) 139.
[34] E.L. Chronister, T.H. Morton, J. Am. Chem. Soc. 112 (1990) 133.
[35] H.W. Zappey, S. Ingemann, N.M.M. Nibbering, J. Chem. Soc. Perkin Trans. 2 (1991) 1887.

[36] S. Olivella, A. Solé, D.J. McAdoo, L.L. Griffin, J. Am. Chem. Soc. 116 (1994) 11078.
[37] J.C. Traeger, C.E. Hudson, D.J. McAdoo, J. Am. Soc. Mass Spectrom. 7 (1996) 73.
[38] L.L. Griffin, K. Holden, C.E. Hudson, D.J. McAdoo, Org. Mass Spectrom. 21 (1986) 175.
[39] B.F. Yates, L. Radom, J. Am. Chem. Soc. 109 (1987) 2910.
[40] C. Walling, in: P. de Mayo (Ed.), Molecular Rearrangements, Interscience, NY, 1963, p. 407.
[41] L.B. Harding, J. Am. Chem. Soc. 103 (1981) 7469.
[42] W. Koch, B. Liu, J. Am. Chem. Soc. 111 (1989) 3479.
[43] C.E. Hudson, D.J. McAdoo, Int. J. Mass Spectrom. 214 (2002) 315.
[44] D.G.I. Kingston, J.T. Bursey, M.M. Bursey, Chem. Rev. 74 (1974) 215.